



THE UNIVERSITY *of* EDINBURGH

Edinburgh Research Explorer

Nutrient cycling in the Atlantic basin: the evolution of nitrate isotope signatures in water masses

Citation for published version:

Tuerena, R, Ganeshram, R, Geibert, W, Fallick, A, Dougans, J, Tait, A, Henley, S & Woodward, M 2015, 'Nutrient cycling in the Atlantic basin: the evolution of nitrate isotope signatures in water masses', *Global Biogeochemical Cycles*, vol. 29, no. 10, pp. 1830–1844. <https://doi.org/10.1002/2015GB005164>

Digital Object Identifier (DOI):

[10.1002/2015GB005164](https://doi.org/10.1002/2015GB005164)

Link:

[Link to publication record in Edinburgh Research Explorer](#)

Document Version:

Publisher's PDF, also known as Version of record

Published In:

Global Biogeochemical Cycles

General rights

Copyright for the publications made accessible via the Edinburgh Research Explorer is retained by the author(s) and / or other copyright owners and it is a condition of accessing these publications that users recognise and abide by the legal requirements associated with these rights.

Take down policy

The University of Edinburgh has made every reasonable effort to ensure that Edinburgh Research Explorer content complies with UK legislation. If you believe that the public display of this file breaches copyright please contact openaccess@ed.ac.uk providing details, and we will remove access to the work immediately and investigate your claim.



RESEARCH ARTICLE

10.1002/2015GB005164

Key Points:

- Atlantic N cycling processes investigated using dual nitrate isotopes
- N recycling and high N:P remineralization observed in subtropics from N fixation
- NADW isotope signatures affected by subtropical Atlantic N recycling

Supporting Information:

- Figures S1–S3

Correspondence to:

R. E. Tuerena,
robyn.tuerena@liverpool.ac.uk

Citation:

Tuerena, R. E., R. S. Ganeshram, W. Geibert, A. E. Fallick, J. Dougans, A. Tait, S. F. Henley, and E. M. S. Woodward (2015), Nutrient cycling in the Atlantic basin: The evolution of nitrate isotope signatures in water masses, *Global Biogeochem. Cycles*, 29, 1830–1844, doi:10.1002/2015GB005164.

Received 10 APR 2015

Accepted 2 OCT 2015

Accepted article online 5 OCT 2015

Published online 28 OCT 2015

Nutrient cycling in the Atlantic basin: The evolution of nitrate isotope signatures in water masses

R. E. Tuerena^{1,2}, R. S. Ganeshram¹, W. Geibert^{1,3}, A. E. Fallick⁴, J. Dougans⁴, A. Tait⁴, S. F. Henley¹, and E. M. S. Woodward⁵

¹School of Geosciences, University of Edinburgh, Edinburgh, UK, ²Department of Earth, Ocean, and Ecological Sciences, University of Liverpool, Liverpool, UK, ³Helmholtz Centre for Polar and Marine Research, Alfred Wegener Institute, Bremerhaven, Germany, ⁴Scottish Universities Environmental Research Centre, University of Glasgow, East Kilbride, UK, ⁵Plymouth Marine Laboratory, Plymouth, UK

Abstract A basin-wide transect of nitrate isotopes ($\delta^{15}\text{N}_{\text{NO}_3}$, $\delta^{18}\text{O}_{\text{NO}_3}$), across the UK GEOTRACES 40°S transect in the South Atlantic is presented. This data set is used to investigate Atlantic nutrient cycling and the communication pathways of nitrogen cycling processes in the global ocean. Intermediate waters formed in the subantarctic are enriched in $\delta^{15}\text{N}_{\text{NO}_3}$ and $\delta^{18}\text{O}_{\text{NO}_3}$ from partial utilization of nitrate by phytoplankton and distant denitrification processes, transporting heavy isotope signatures to the subtropical Atlantic. Water mass modification through the Atlantic is investigated by comparing data from 40°S (South Atlantic) and 30°N (North Atlantic). This reveals that nitrate in the upper intermediate waters is regenerated as it transits through the subtropical Atlantic, as evidenced by decreases in $\delta^{18}\text{O}_{\text{NO}_3}$. We document diazotrophy-producing high N:P particle ratios (18–21:1) for remineralization, which is further confirmed by a decrease in $\delta^{15}\text{N}_{\text{NO}_3}$ through the subtropical Atlantic. These modifications influence the isotopic signatures of the North Atlantic Deep Water (NADW) which is subsequently exported from the Atlantic to the Southern Ocean. This study reveals the dominance of recycling processes and diazotrophy on nitrate cycling in the Atlantic. These processes provide a source of low $\delta^{15}\text{N}_{\text{NO}_3}$ to the Southern Ocean via the NADW, to counteract enrichment in $\delta^{15}\text{N}_{\text{NO}_3}$ from water column denitrification in the Indo/Pacific basins. We hence identify the Southern Ocean as a key hub through which denitrification and N_2 fixation communicate in the ocean through deepwater masses. Therefore, the balancing of the oceanic N budget and isotopic signatures require time scales of oceanic mixing.

1. Introduction

Nitrate (NO_3^-) is an essential nutrient for marine phytoplankton and limits primary production in much of the global ocean. The supply of NO_3^- to the surface ocean therefore has implications on the efficiency of the biological pump and CO_2 regulation. Denitrification and N_2 fixation by diazotrophs are the main sink and source of NO_3^- in the ocean and hence exert a predominant control on the ocean NO_3^- inventory and mass balance [Gruber, 2004]. Nevertheless, these processes are spatially separated in the ocean. Water column denitrification at globally significant rates occurs in the northern Indian and eastern Pacific Ocean basins. N_2 fixation may occur distributed over the tropics and subtropics and is determined by the availability of excess phosphate (P) and iron (Fe) [Deutsch et al., 2007; Moore et al., 2009].

In the South Atlantic, deep waters that originate from the Pacific and Southern Oceans meet with those of North Atlantic origin. This confluence makes the ideal location to investigate the water mass pathways through which oceanic N loss and gain communicate by documenting contrasting nutrient properties in water masses. Of particular significance is the Upper Circumpolar Deep Water (UCDW) which is sourced from the Antarctic Circumpolar Current (ACC), where deep waters from Atlantic, Pacific, and Indian Ocean basins are added on its eastward circumpolar circuit [Oudot et al., 1999]. The UCDW has the potential to carry isotopic signatures of N processing from other ocean basins into the Atlantic basin. The Antarctic Intermediate Water (AAIW) and Subantarctic Mode Water (SAMW) overlay the UCDW in the Atlantic and are principally formed from UCDW. In the Atlantic Ocean, they undergo modification at the ocean surface during ventilation and northward transport [Piola and Georgi, 1982; Sloyan and Rintoul, 2001]. Together these Antarctic intermediate waters set the baseline nutrient conditions and isotopic signatures which are transferred to the Atlantic thermocline [Sarmiento et al., 2004]. The Antarctic Bottom Water (AABW) is also sourced from the Southern Ocean and is

©2015. The Authors.

This is an open access article under the terms of the Creative Commons Attribution License, which permits use, distribution and reproduction in any medium, provided the original work is properly cited.

the densest of oceanic water masses [Orsi *et al.*, 1999]. Its formation is centered on the Antarctic continental margins where Circumpolar Deep Water (CDW) is entrained southward from the ACC, interacting with cold and dense shelf waters [Naveira Garabato *et al.*, 2002]. The AABW is transported northward into the abyssal plains of the South Atlantic and feeds Atlantic deepwater formation.

In the Atlantic, the northward flow of Antarctic intermediate and bottom waters feed the formation of the North Atlantic Deep Water (NADW), which ventilates the global ocean. The NADW provides approximately half of the deep waters of the global ocean and has higher N:P concentrations compared to Southern Ocean deep waters [Gruber and Sarmiento, 1997]. These differences may be attributed to the spatial segregation between denitrification and N_2 fixation in the ocean. The Atlantic Ocean is thought to be where N_2 fixation may exceed denitrification. The negligible N loss may feed a net export of N from the Atlantic Ocean through NADW transport [Moore *et al.*, 2009]. In contrast, water masses from the ACC such as the UCDW and the associated SAMW and AAIW have the potential to carry a denitrification signal from the Pacific and Indian Oceans to be modified during northward transport under the Atlantic thermocline. In this study we use isotopic signatures of NO_3^- in the South Atlantic to investigate the water mass pathways through which the processes of N loss and gain communicate through the global Meridional Overturning Circulation (MOC). We attempt to further clarify the degree to which the Atlantic N cycle is internally balanced. This has important implications to the time scales over which source and sink terms in the global oceanic N budget are balanced and the response time of the N cycle to anthropogenic perturbations such as the expansion of denitrification zones in response to global change [Kalvelage *et al.*, 2013; Weber and Deutsch, 2014].

The $^{15}N/^{14}N$ and $^{18}O/^{16}O$ of NO_3^- are sensitive to biogeochemical cycling and can indicate the origin and modification of water masses [Sigman *et al.*, 2000]. N and O isotope signatures in NO_3^- ($\delta^{15}N_{NO_3}$ and $\delta^{18}O_{NO_3}$) can be used as integrative tracers of N cycling processes which may vary temporally and spatially within the ocean [e.g., DiFiore *et al.*, 2006; Rafter *et al.*, 2013]. Isotope ratios are measured relative to a reference (AIR, Vienna Standard Mean Ocean Water (VSMOW)) and are expressed in a delta notation ($\delta^{15}N$ versus AIR (‰) = $(R_{sam}/R_{std} - 1) \times 1000$ and $\delta^{18}O$ versus VSMOW (‰) = $(R_{sam}/R_{std} - 1) \times 1000$). The isotopic effect (defined here in per mil notation as $\epsilon = ^{15}K/^{14}K - 1$, where ^{14}K and ^{15}K are the rate coefficients of ^{14}N and ^{15}N) of N cycling processes leaves an isotopic “fingerprint” on NO_3^- within water masses. The integrated nature of isotopic signatures helps to avoid the complexities in upscaling shipboard measurements of variable N cycling processes and assumptions in modelling estimates [Sigman *et al.*, 2009a].

The average subsurface oceanic $\delta^{15}N_{NO_3}$ is close to 5‰ and globally can be interpreted as a balance between isotopic fractionation during N_2 fixation and denitrification [Brandes and Devol, 2002; Sigman *et al.*, 2009a]. Nitrate consumption by phytoplankton acts to enrich the residual pool of NO_3^- in ^{15}N , with an isotopic effect of $\sim 5\text{‰}$ [Altabet and Francois, 2001]. In the subtropical gyres, NO_3^- is fully consumed by phytoplankton; therefore, uptake and remineralization have minimal effect on subsurface $\delta^{15}N_{NO_3}$, as remineralized organic N should equal the NO_3^- source [Sigman *et al.*, 2000]. In the Southern Ocean, NO_3^- remains high in surface waters from low light levels and iron limitation [e.g., Boyd *et al.*, 2007]. Here partial utilization of macronutrients leaves an isotopic imprint in surface waters as NO_3^- (higher ^{15}N and ^{18}O with decreasing NO_3^-) which is then transferred to Southern Ocean-sourced intermediate waters as preformed signatures [Sigman *et al.*, 2000]. In these water masses, changes in the isotopic signatures may indicate the importance of both physical mixing and biogeochemical changes during water mass formation.

The $\delta^{15}N_{NO_3}$ can be indicative of processes far beyond the localized regions of water mass formation or NO_3^- input/output. Nitrate added to the ocean by N_2 fixation is not fractionated during atmospheric N_2 uptake [Carpenter *et al.*, 1997]. Therefore, newly fixed N in organic matter has light isotope signatures, comparable to the dissolved N_2 source (~ -1 to 0‰) [Brandes and Devol, 2002]. Remineralization of diazotrophic material adds NO_3^- to the water column which is relatively depleted in ^{15}N compared to mean subsurface NO_3^- . The isotope effect of water column denitrification is $20\text{--}30\text{‰}$ [Brandes *et al.*, 1998; Altabet *et al.*, 1999], and N loss during this process leaves an isotopically enriched imprint on $\delta^{15}N_{NO_3}$.

The O isotopes of NO_3^- are consumed with a similar isotopic effect to N ($^{15}\epsilon = ^{18}\epsilon$) for both algal consumption and denitrification during the process of NO_3^- reduction [Granger *et al.*, 2004; Karsh *et al.*, 2012]. Therefore, as denitrification or NO_3^- utilization occurs, $\delta^{15}N_{NO_3}$ and $\delta^{18}O_{NO_3}$ become increasingly higher along a 1:1 trajectory [DiFiore *et al.*, 2009; Sigman *et al.*, 2009b]. In contrast, the production of NO_3^- has different effects

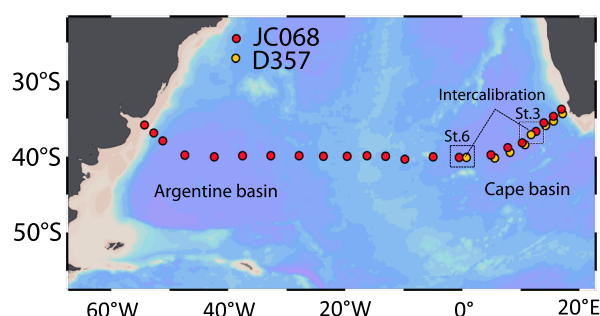


Figure 1. The UK GEOTRACES 40°S transect across the South Atlantic. Samples were collected in an EW transect from Cape Town to Montevideo. Stations sampled from D357 (October to November 2010) are highlighted in yellow and JC068 (December 2011 to January 2012) are highlighted in red. Stations 3 and 6 were cross-comparison stations between the two cruises.

bility in $\delta^{18}\text{O}$ of seawater, reflecting mainly salinity in the deep ocean, nitrification produces a relatively homogenous $\delta^{18}\text{O}_{\text{NO}_3}$ signature [Buchwald *et al.*, 2012]. The newly nitrified $\delta^{18}\text{O}_{\text{NO}_3}$ therefore loses any previous enrichment from denitrification or partial utilization processes, and the small isotopic range of $\delta^{18}\text{O}$ contrasts the variability in $\delta^{15}\text{N}$ supplied to nitrification. This difference allows their coupled measurement to isolate the importance of processes such as NO_3^- utilization, which fractionates both isotopes equally, and nitrification processes, which produces distinct signatures [Sigman *et al.*, 2005; Smart *et al.*, 2015].

The difference in the processes that form NO_3^- for N and O atoms has led to their dual measurement and the development of the parameter $\Delta(15-18)$ (defined here as $\delta^{15}\text{N}_{\text{NO}_3} - \delta^{18}\text{O}_{\text{NO}_3}$) [Rafter *et al.*, 2013]. $\Delta(15-18)$ is used in NO_3^- isotope studies to identify the different sources of remineralized NO_3^- [Knapp *et al.*, 2008]. A deviation away from a 1:1 relationship in $\delta^{15}\text{N}_{\text{NO}_3}$ and $\delta^{18}\text{O}_{\text{NO}_3}$, and therefore shift in $\Delta(15-18)$, gives information about how NO_3^- was formed. A lowering of $\Delta(15-18)$ indicates the addition of low ^{15}N , i.e., by remineralization of newly fixed organic matter ($\delta^{15}\text{N} \sim -1\text{‰}$, $\delta^{18}\text{O} \sim -1.1\text{‰}$) and a high $\Delta(15-18)$ can represent remineralization in NO_3^- depleted areas ($\delta^{15}\text{N} \sim 5\text{‰}$, $\delta^{18}\text{O} \sim 1.1\text{‰}$). This geochemical proxy has been used to estimate rates of N_2 fixation [Knapp *et al.*, 2008], redox recycling processes [Sigman *et al.*, 2005], and N regeneration over ocean basin scales [Rafter *et al.*, 2013].

In this study, we present a full zonal transect of the $\delta^{15}\text{N}_{\text{NO}_3}$ and $\delta^{18}\text{O}_{\text{NO}_3}$ in the South Atlantic Ocean at 40°S as part of UK GEOTRACES (Figure 1). This section allows the characterization of the basin-scale import of NO_3^- through the Southern Ocean water masses and the export of NO_3^- in the NADW. We use $\delta^{15}\text{N}_{\text{NO}_3}$ and $\delta^{18}\text{O}_{\text{NO}_3}$ data to disentangle the processes of their formation and modification during transport and the nutrient biogeochemistry of the Atlantic Ocean. The formation of AABW and intermediate waters are investigated, and their characterization provides information on their modification in the Atlantic basin. The isotopic effect of NO_3^- regeneration on subsurface water masses during transit in the subtropical Atlantic is investigated by comparing $\delta^{18}\text{O}_{\text{NO}_3}$ from this study with previously published data from the Sargasso Sea [Knapp *et al.*, 2008]. Nitrate isotope signatures of the NADW being exported from the Atlantic basin are compared with deepwater mass signatures of the Pacific and Indian basins. These data are used to describe the water mass pathways through which oceanic N loss and gain are communicated through the global Meridional Overturning Circulation (MOC).

2. Methods

Samples were collected on board the Royal Research Ship (RRS) *Discovery* between October and November 2010 (D357) and the RRS *James Cook* between December 2011 and February 2012 (JC068) as part of the UK GEOTRACES 40°S transect (<http://www.ukgeotraces.com>). On both cruises, samples were collected on an east to west transect, with full water column sampling at each station. The transect captures collectively the Cape and Argentine basins of the South Atlantic, allowing full characterization of the water mass structure (Figure 1). The two cruise legs were intercalibrated with two repeat stations of the full water column, which showed comparable nutrient concentrations and isotope abundances (within 1σ) below 500 m; seasonal differences were observed above this depth when comparing the two cruises. Samples in the upper 500 m were solely used from JC068

on $\delta^{15}\text{N}_{\text{NO}_3}$ and $\delta^{18}\text{O}_{\text{NO}_3}$. N atoms are obtained from the available fixed N pool at the time of nitrification, the isotopic values may therefore be highly variable depending on the internal N cycling occurring in the water column. During nitrification, O atoms are sourced principally from water molecules [Buchwald *et al.*, 2012], which produces a signature of $\sim 1.1\text{‰}$ above the in situ $\delta^{18}\text{O}$ of seawater [Sigman *et al.*, 2009a]. The $\delta^{18}\text{O}_{\text{H}_2\text{O}}$ of seawater is relatively homogenous, with typical values for the global ocean between -0.4 and 0.5‰ [Bigg and Rohling, 2000]. Given the small range of varia-

Table 1. Water Mass Properties at 40°S in the South Atlantic as Identified by Density [See *Stramma and England, 1999*]

Water Mass	Temperature (°C)	Salinity (psu)	Density (kg m^{-3})	$\delta^{15}\text{N}_{\text{NO}_3}$ (‰)	$\delta^{18}\text{O}_{\text{NO}_3}$ (‰)	AOU ($\mu\text{mol kg}^{-1}$)
AABW	0.7	34.8	28.3	4.8	2.0	131.8
NADW	2.7	34.8	28.0	4.8	2.0	112.7
UCDW	3.1	34.5	27.6	5.4	2.4	140.3
AAIW	4.3	34.3	27.3	5.9	3.0	86.1
SAMW	6.3	34.6	27.1	6.2	3.4	74.3

to overcome seasonal variability. Nitrate plus nitrite concentrations (herein referred to as NO_3^-) were determined using an AA III segmented flow Auto Analyzer (Bran and Luebbe) following standard colorimetric procedures [Woodward and Rees, 2001]. Clean sample handling and laboratory techniques were adopted according to Global Ocean Ship-based Hydrographic Investigations Program nutrient protocols [Hydes *et al.*, 2010], and all samples were analyzed as soon after sampling as possible; no samples were stored. Salinity, temperature, and depth were measured using a CTD system (Seabird 911+), and salinity was calibrated onboard with discrete samples using an Autosol 8400B salinometer (Guildline). Dissolved O_2 from the CTD was determined by a Seabird SBE 43 O_2 sensor and calibrated using a photometric automated Winkler titration system [Carritt and Carpenter, 1966].

Water samples for NO_3^- isotope analysis were collected from a stainless steel rosette; seawater was filtered through an online Acropak filter (0.4 μm) into HCl clean 60 ml Nalgene bottles and frozen at -20°C . Nitrate $\delta^{15}\text{N}$ and $\delta^{18}\text{O}$ were determined by the bacterial conversion of NO_3^- to N_2O via the denitrifier method using denitrifier strain *Pseudomonas aureofaciens* [Sigman *et al.*, 2001; Casciotti *et al.*, 2002; McIlvin and Casciotti, 2011]. Sample analysis was carried out at the Scottish Universities Environmental Research Centre (SUERC) and The University of Edinburgh following GEOTRACES intercalibration techniques (<http://www.geotrac.es.org/images/stories/documents/intercalibration/Cookbook.pdf>). Isotopic analysis was carried out at SUERC using a custom-built gas chromatography–isotope ratio mass spectrometry system in line with a VG Prism III isotope ratio mass spectrometer. Sample analysis at the University of Edinburgh used a Gasbench II coupled with a Delta + Advantage. On both instruments, isotopic measurements of sample N_2O were measured relative to a reference peak. Absolute measurements of $\delta^{15}\text{N}_{\text{NO}_3}$ and $\delta^{18}\text{O}_{\text{NO}_3}$ were corrected to AIR and VSMOW, respectively, with the use of international reference standards N3, USGS32, USGS34, and USGS35 [Böhlke *et al.*, 2003]. One blank and all standards (run in triplicate) were analyzed in every batch and analytical precision at 1σ for reference material was typically $\pm 0.2\text{‰}$ for $\delta^{15}\text{N}$ and $\pm 0.3\text{‰}$ for $\delta^{18}\text{O}$.

The stoichiometric parameter N^* is calculated here as $\text{NO}_3^- - 16 \times \text{PO}_4^{3-}$ [Gruber and Sarmiento, 1997]. Proportions of remineralized and preformed phosphate were calculated using apparent oxygen utilization (AOU) ($\text{AOU} = [\text{O}_2]_{\text{sat}} - [\text{O}_2]_{\text{observed}}$). These were converted to NO_3^- using organic matter respiration stoichiometry ([Anderson, 1995], $[\text{PO}_4^{3-}]_{\text{remin}} = 1/150 \times \text{AOU}$; $[\text{PO}_4^{3-}]_{\text{preformed}} = [\text{PO}_4^{3-}]_{\text{observed}} - [\text{PO}_4^{3-}]_{\text{remin}}$).

3. Results

The 40°S transect captures the deepwater masses which are transported through the Cape and Argentine basins (Figure 1); these are identified using the densities and salinities discussed in *Stramma and England, 1999* (Table 1). The densest of the water masses at 40°S is the Weddell Sea Deep Water (WSDW), identified in the Argentine basin with temperatures below 0°C (Figure 2). Overlying this, the Lower Circumpolar Deep Water (LCDW) formed in the Antarctic Circumpolar Current (ACC) is identified below 3500 m by temperatures between 0 and 1.5°C in the Cape and Argentine basins. The WSDW and LCDW have similar nutrient properties and together comprise the Antarctic Bottom Water (AABW), with a density of $\sim 28.3 \text{ kg m}^{-3}$ (Figure 3). At 40°S, the southward flowing NADW has a salinity of 34.8 practical salinity unit (psu); its core has been eroded by the entrainment of Southern Ocean waters but is still evident on the western boundary with higher salinities (up to 34.9 psu) (Figures 2 and 3). The Upper Circumpolar Deep Water (UCDW), originating from the ACC, is detectable with a core at a depth of 1250 m and a density of 27.6 kg m^{-3} . Above the UCDW, the less dense Antarctic Intermediate Water (AAIW) and Subantarctic Mode Water (SAMW) have lower salinities and are ventilated in the subantarctic surface. The AAIW is formed at the Subantarctic Front (SAF) and has a salinity minimum at 750 m (~ 34.2 psu), a consequence of high precipitation rates and sea ice in

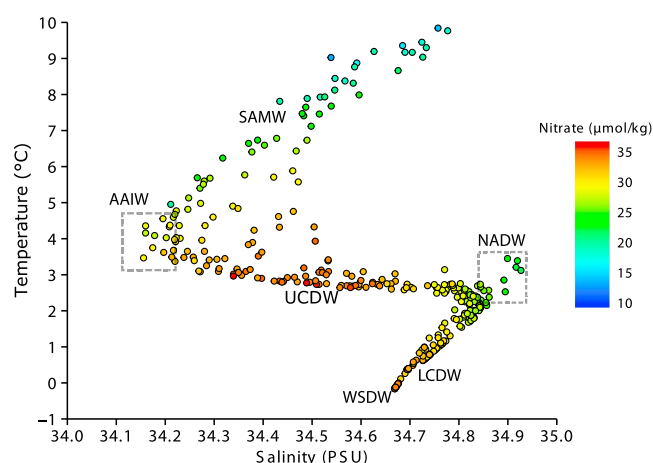


Figure 2. Temperature versus salinity showing water mass structure at 40°S with symbol color by NO_3^- .

formation regions at ~55°S [Talley, 1996]. Overlying the AAIW is the SAMW which is formed in a deep winter-mixed layer in the SE Pacific. These waters enter the Atlantic via the Drake Passage; at 40°S, the core of this water mass is at 500 m detectable with a density of $\sim 27.1 \text{ kg m}^{-3}$.

The subsurface waters of the South Atlantic are well oxygenated with O_2 concentrations above $\sim 175 \mu\text{M}$. The lowest O_2 concentrations and highest AOU concentrations are found in the UCDW (Figure 3), which has been enhanced with remineralized nutrients from the Pacific and Indian Oceans, and from its transit within the ACC. In

contrast, the AAIW and SAMW have much lower AOU concentrations, as they are newly formed within the subantarctic surface. The LCDW and WSDW have high macronutrient concentrations retained from their formation regions, with NO_3^- typically $> 30 \mu\text{M}$; their isotopic properties are indistinguishable and therefore are discussed collectively henceforth as the AABW (Figure 3 and Figure S1 in the supporting information). The AABW can be identified with $\delta^{15}\text{N}_{\text{NO}_3}$ of $4.8\text{‰} \pm 0.2$ and $\delta^{18}\text{O}_{\text{NO}_3}$ of $2.0\text{‰} \pm 0.2$ (Figure 4). In contrast, low-nutrient surface waters dilute the NO_3^- concentration of NADW during formation (Figure 3). The average NADW $\delta^{15}\text{N}_{\text{NO}_3}$ and $\delta^{18}\text{O}_{\text{NO}_3}$ are $4.8 \pm 0.2\text{‰}$ and $2.0 \pm 0.2\text{‰}$, respectively; these values are similar to the underlying AABW but lower than the UCDW (Figure 4).

In the UCDW, $\delta^{15}\text{N}_{\text{NO}_3} = 5.4 \pm 0.2\text{‰}$, which is slightly enriched above deep ocean NO_3^- signatures. The $\delta^{18}\text{O}_{\text{NO}_3}$ is also slightly enriched compared to the underlying water masses, with average values of $2.4 \pm 0.2\text{‰}$. Enrichment in $\delta^{15}\text{N}_{\text{NO}_3}$ has been identified in previous work [Sigman *et al.*, 2000] and has been attributed to communication with areas of denitrification. The Atlantic AAIW and the SAMW are both formed north of the Polar Front in the Pacific Ocean. The AAIW which forms at the Subantarctic Front (SAF) has high NO_3^- concentrations, $\sim 3 \mu\text{M}$ lower than the UCDW (Figure 3). This decrease in NO_3^- coincides with an enrichment in $\delta^{15}\text{N}_{\text{NO}_3}$ and $\delta^{18}\text{O}_{\text{NO}_3}$ of the AAIW following an isotopic effect of 5‰ for NO_3^- utilization (Figure 4). The SAMW at 40°S is within the nutricline at $\sim 500 \text{ m}$ (Figure 3), demonstrating variable concentrations, which decrease toward the surface. In Rayleigh space ($\ln(\text{NO}_3^-)$ versus $\delta^{15}\text{N}_{\text{NO}_3}/\delta^{18}\text{O}_{\text{NO}_3}$, see Figure 4), SAMW $\delta^{15}\text{N}_{\text{NO}_3}$ falls below the utilization trend when compared to the UCDW and the AAIW. The $\delta^{18}\text{O}_{\text{NO}_3}$ follows a similar trend to $\delta^{15}\text{N}_{\text{NO}_3}$, although $\delta^{18}\text{O}_{\text{NO}_3}$ is less decoupled from the Rayleigh trend. In the forthcoming sections, the NO_3^- isotope signatures in these water masses will be discussed and the processes by which they originate investigated.

4. Discussion

4.1. Formation of Southern Ocean Water Masses

4.1.1. Antarctic Bottom Water

At 40°S, AABW exhibits a $\delta^{15}\text{N}_{\text{NO}_3}$ of $4.8 \pm 0.2\text{‰}$ and $\delta^{18}\text{O}_{\text{NO}_3}$ of $2.0 \pm 0.2\text{‰}$ (Figure 3). The isotopic signatures are comparable to those reported in the Indian and Pacific sectors of the Southern Ocean [$\delta^{15}\text{N}_{\text{NO}_3} = 4.8 \pm 0.2\text{‰}$, $\delta^{18}\text{O}_{\text{NO}_3} = 1.8 \pm 0.2\text{‰}$, Sigman *et al.*, 2000, 2009a; Rafter *et al.*, 2013]. Previous studies have attributed the isotopically lighter signature of Pacific AABW to mixing with NADW [Rafter *et al.*, 2013]. The $\delta^{18}\text{O}_{\text{NO}_3}$ of NADW at 40°S (2.0‰) is too high to produce the low $\delta^{18}\text{O}_{\text{NO}_3}$ reported in the Southern Ocean AABW (1.6‰); therefore, these low signatures may be produced by remineralization processes. Recent work has identified low $\delta^{18}\text{O}_{\text{NO}_3}$ in the Kerguelen Plateau area of the Southern Ocean, which has been attributed to nitrification [Dehairs *et al.*, 2015]. This may suggest that nitrification processes may be prevalent in some regions of the Southern Ocean, causing the decreases in $\delta^{18}\text{O}_{\text{NO}_3}$ to lower values in Southern Ocean-sourced deepwater masses [Rafter *et al.*, 2013; Dehairs *et al.*, 2015].

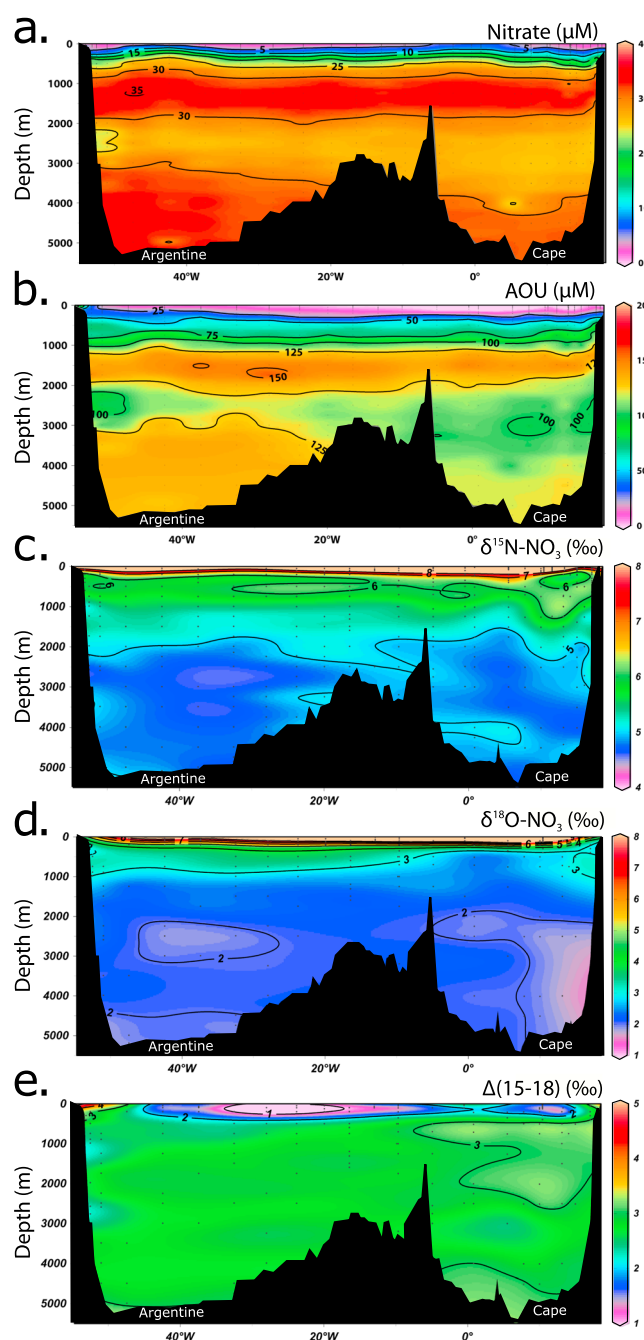


Figure 3. Full depth transects across 40°S. Sections of (a) NO_3^- in μM , (b) apparent oxygen utilization (AOU) in μM , $\text{AOU} = [\text{O}_2]_{\text{sat}} - [\text{O}_2]$ observed, (c) $\delta^{15}\text{N}_{\text{NO}_3}$ (‰ versus AIR), (d) $\delta^{18}\text{O}_{\text{NO}_3}$ (‰ versus VSMOW), and (e) $\Delta(15-18)$ (defined as $\delta^{15}\text{N}_{\text{NO}_3} - \delta^{18}\text{O}_{\text{NO}_3}$).

Southern Ocean, the effect of remineralization on the overall water mass signature is low in comparison to the enrichment observed by denitrification in distant regions. This is consistent with the high nutrient concentrations in the CDW requiring a large amount of remineralized NO_3^- to make a significant change to isotopic signatures.

4.1.3. Antarctic Intermediate Water

At 40°S, NO_3^- is found to decrease from the UCDW to the AAIW, which coincides with an increase in $\delta^{15}\text{N}_{\text{NO}_3}$ and $\delta^{18}\text{O}_{\text{NO}_3}$ to 5.9‰ and 3.0‰, respectively (Figure 4 and Table 1). The enrichment in $\delta^{15}\text{N}_{\text{NO}_3}$ and $\delta^{18}\text{O}_{\text{NO}_3}$

4.1.2. Upper Circumpolar Deep Water

At 40°S, $\delta^{15}\text{N}_{\text{NO}_3}$ and $\delta^{18}\text{O}_{\text{NO}_3}$ are found to be enriched above typical deep ocean values to ~5.4‰ and ~2.4‰, respectively (Table 1 and Figure 5). These values are comparable to $\delta^{15}\text{N}_{\text{NO}_3}$ of ~5.5‰ reported for this water mass in the Pacific/Indian sectors of the Southern Ocean [Sigman *et al.*, 2000]. This relatively enriched value of UCDW over the global ocean average (~4.8‰) is attributed to the incorporation of ^{15}N -enriched NO_3^- via interactions with ODZs (Oxygen Deficient Zones) [Sigman *et al.*, 2000], although slightly lower values of 5‰ and 2‰ for $\delta^{15}\text{N}_{\text{NO}_3}$ and $\delta^{18}\text{O}_{\text{NO}_3}$, respectively, were also reported in the Pacific UCDW due to modifications during transport [Rafter *et al.*, 2013]. The loss of NO_3^- via denitrification leaves an imprint on $\delta^{15}\text{N}_{\text{NO}_3}$ and $\delta^{18}\text{O}_{\text{NO}_3}$, which is then transported far from the ODZ where the process occurred [Sigman *et al.*, 2000]. Thus, the high $\delta^{15}\text{N}_{\text{NO}_3}$ isotopic characteristics of the UCDW are inherited from the Pacific and Indian Oceans, transporting a denitrification signal into the Atlantic Ocean, which can be further supported by low O_2 and N^* concentrations.

The $\Delta(15-18)$ of Pacific UCDW has been measured at 3‰ and appears to be unaltered by NO_3^- utilization and remineralization at the Southern Ocean surface [Rafter *et al.*, 2013]; in this study the $\Delta(15-18)$ is comparable (3‰), which can further suggest a negligible effect of nitrification on this isopycnal. It is expected that sinking organic matter in NO_3^- -rich Southern Ocean surface waters would add lower $\delta^{15}\text{N}_{\text{NO}_3}$ and low $\Delta(15-18)$ to the underlying water mass through remineralization. As there is no observed decrease in $\Delta(15-18)$ during water mass transit from the

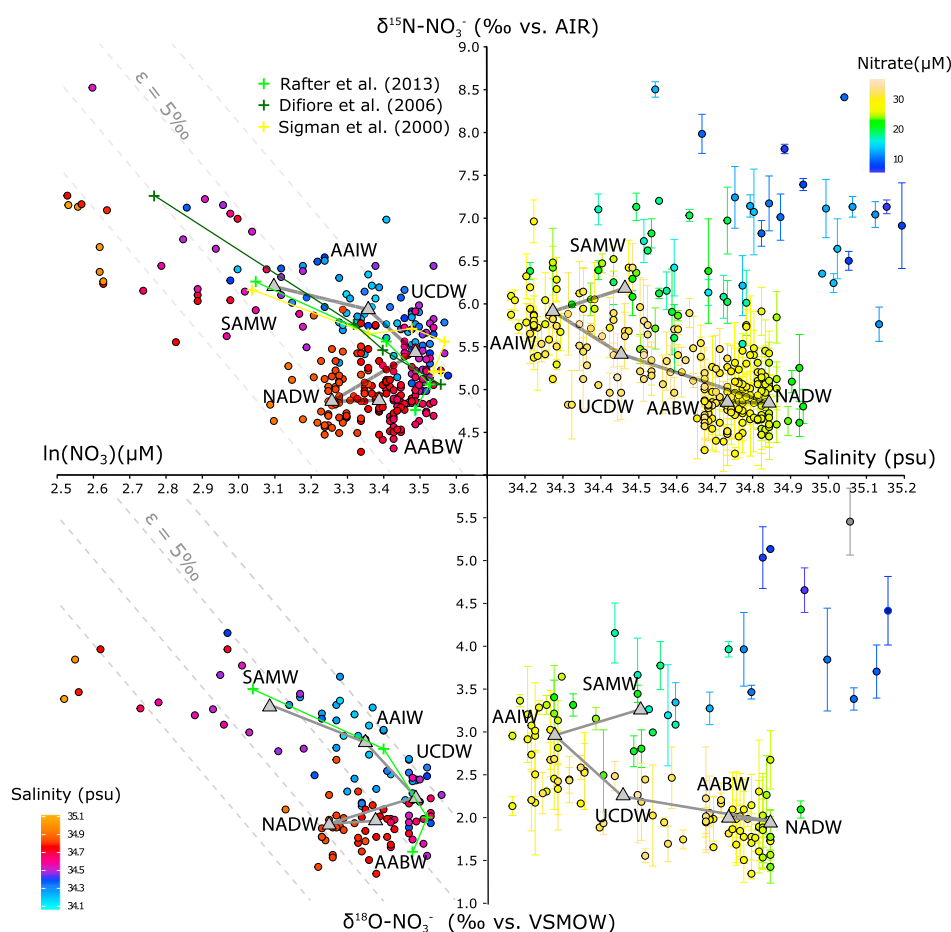


Figure 4. The (a) $\delta^{15}\text{N}_{\text{NO}_3^-}$ and (b) $\delta^{18}\text{O}_{\text{NO}_3^-}$ plotted against $\ln(\text{NO}_3^-)$ and salinity. Average values for each water mass are plotted with grey triangles; these are calculated by using the core depth of each water mass at 40°S . (WSDW = 4500 m, LCDW = 4000 m, NADW = 2500 m, UCDW = 1250 m, AAIW = 750 m, and SAMW = 500 m). (left) Comparison of the isotopic properties of water masses at 40°S in Rayleigh space. The grey dashed lines mark a fractionation trend (ϵ) of 5‰. (right) Changes in isotopic signatures with the salinity of the water mass.

follows an isotopic effect of $\sim 5\text{‰}$, indicating that the NO_3^- decrease in this water mass is from the consumption of NO_3^- by phytoplankton at the SAZ surface. This suggests that the AAIW is formed principally from the UCDW and Antarctic Surface Water (AASW) (which is also formed from the UCDW) and partial NO_3^- assimilation in the AASW drives increases in both $\delta^{15}\text{N}_{\text{NO}_3^-}$ and $\delta^{18}\text{O}_{\text{NO}_3^-}$ along a NO_3^- utilization fractionation trend. These elevations in $\delta^{15}\text{N}_{\text{NO}_3^-}$ and $\delta^{18}\text{O}_{\text{NO}_3^-}$ have been observed in the summer SAZ surface [Rafter *et al.*, 2013], and subsequent winter mixing and formation of the AAIW drive the incorporation of this elevated $\delta^{15}\text{N}_{\text{NO}_3^-}$ and $\delta^{18}\text{O}_{\text{NO}_3^-}$ into the AAIW. The $\Delta(15-18)$ of AAIW is comparable to the UCDW (2.9‰), which indicates that isotopically lighter N added by the remineralization of organic matter from the SAZ does not significantly alter the signature [Rafter *et al.*, 2013].

4.1.4. Subantarctic Mode Water

In contrast to the AAIW, the overlying SAMW falls off the Rayleigh trend of NO_3^- consumption, as shown in Figure 4. The SAMW has a lower $\delta^{15}\text{N}/\text{NO}_3^-$ relationship compared to other Southern Ocean water masses, which has been attributed to mixing with the subtropical thermocline (Table 1 and Figure 4) [Sigman *et al.*, 2000; DiFiore *et al.*, 2006]. The Atlantic subtropical thermocline has low NO_3^- concentrations but also low $\delta^{15}\text{N}_{\text{NO}_3^-}$ from the addition of newly fixed N, both of which may delineate the SAMW from the Rayleigh relationship. The $\delta^{15}\text{N}_{\text{NO}_3^-}$ at 40°S therefore identifies the importance of subtropical waters in the formation of the Atlantic SAMW.

The $\Delta(15-18)$ signatures within the Atlantic SAMW are lower than the UCDW by $\sim 0.2\text{‰}$. Similarly, the $\Delta(15-18)$ in Pacific SAMW is lower than the UCDW and AAIW [Rafter *et al.*, 2013] and has been attributed to the sinking of

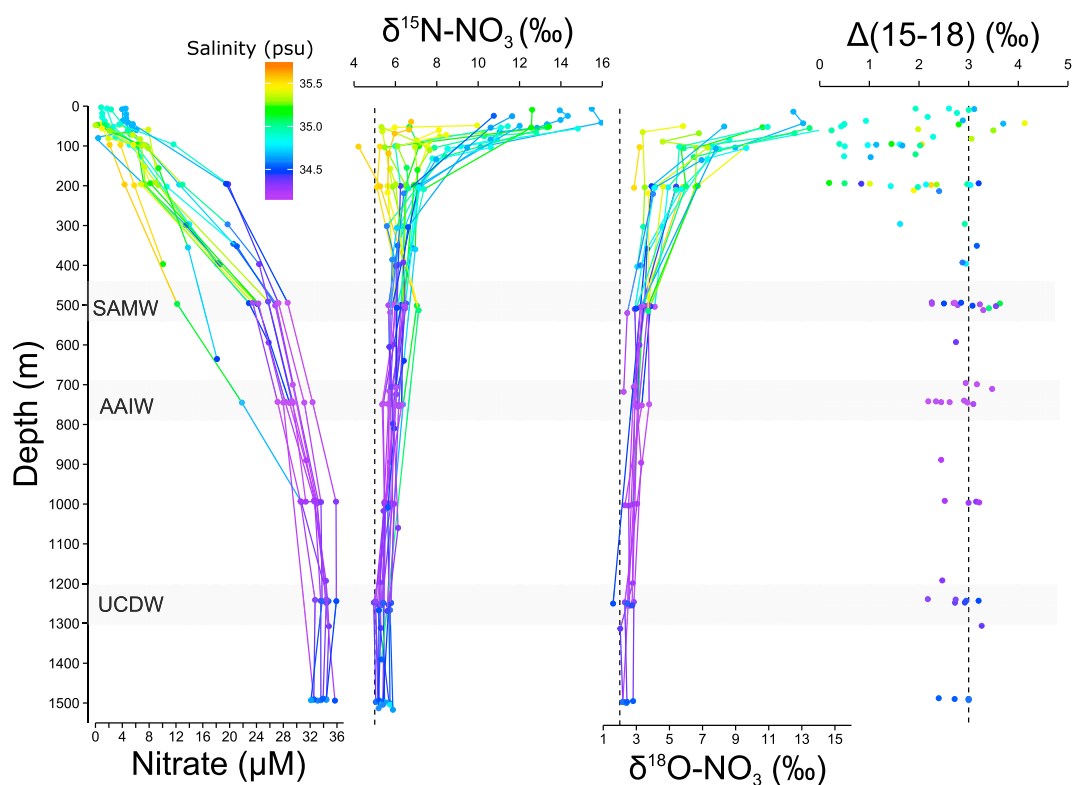


Figure 5. Depth profiles (0–1500 m) of (a) Nitrate (μM), (b) $\delta^{15}\text{N}_{\text{NO}_3}$ (‰ versus AIR), (c) $\delta^{18}\text{O}_{\text{NO}_3}$ (‰ versus VSMOW), and (d) $\Delta(15-18)$ (defined as $\delta^{15}\text{N}_{\text{NO}_3} - \delta^{18}\text{O}_{\text{NO}_3}$). Colors denote salinity (psu). For full water column profile, see Figure S1 in the supporting information.

low- ^{15}N organic matter produced in surface waters, where high NO_3^- concentrations allow the preferential consumption of ^{14}N . The subsurface low $\delta^{15}\text{N}_{\text{NO}_3}$ produced from remineralized NO_3^- is recycled to the surface during winter mixing events. This seasonal cycling in which remineralized NO_3^- with low $\delta^{15}\text{N}$ replenishes the SAMW may be an important component of intermediate water modification [Rafter *et al.*, 2013]. We suggest that the $\Delta(15-18)$ in Atlantic SAMW results from these remineralization processes and also mixing with the low-latitude thermocline.

Characterizing the sources of NO_3^- within the intermediate waters entering the Atlantic is vital for understanding the biogeochemical cycling of NO_3^- within the Atlantic basin. These water masses are an important component of heat and freshwater transport, and their northward transport help to balance the export of the NADW from the Atlantic basin. The UCDW, which is the base of intermediate water formation, has high $\delta^{15}\text{N}_{\text{NO}_3}$ from denitrification and low N^* , hence importing excess P into the Atlantic. The characterization of the UCDW, AAIW, and SAMW can be used as a baseline to investigate the regeneration processes within the upper Atlantic Ocean and the southward export of deep waters from the Atlantic at 40°S in the NADW.

4.2. Modification of Intermediate Waters

In general, enrichments in $\delta^{18}\text{O}_{\text{NO}_3}$ from the processes of partial utilization and denitrification are not expressed in deep ocean NO_3^- . This is because heavy $\delta^{18}\text{O}_{\text{NO}_3}$ signatures inherited from these processes are lost as NO_3^- undergoes biological uptake, regeneration, and nitrification. The subantarctic is one of the only regions where partial NO_3^- utilization by phytoplankton leads to increases in $\delta^{18}\text{O}_{\text{NO}_3}$ in the subsurface (Figure 5). At 40°S , $\delta^{18}\text{O}_{\text{NO}_3}$ ranges between 2.4 and 6.6 ‰ within the density range of 27.6 to 26.5 kg m^{-3} from partial utilization (Figure 6). Nutrient consumption and remineralization of NO_3^- during transit in the low-latitude Atlantic should lead to decreases in $\delta^{18}\text{O}_{\text{NO}_3}$ due to nitrification. The magnitude of such shifts during water mass transits provides a means for documenting and understanding the efficiency of nutrient recycling processes [Toggweiler *et al.*, 1991; Jenkins and Doney, 2003; Sigman *et al.*, 2009a].

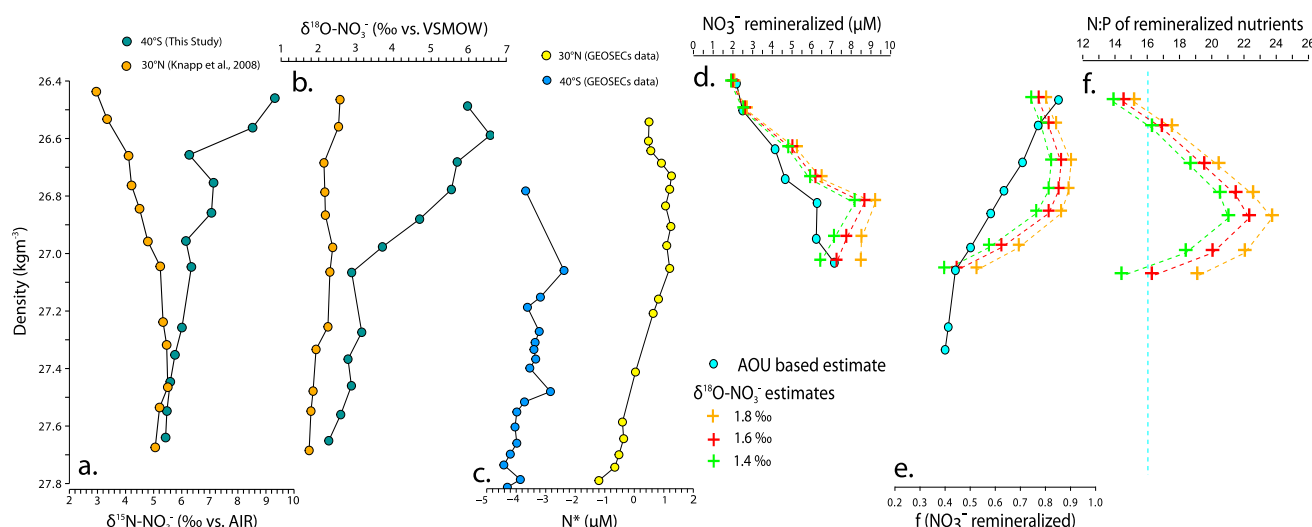


Figure 6. Comparison of (a) $\delta^{15}\text{N}_{\text{NO}_3^-}$, (b) $\delta^{18}\text{O}_{\text{NO}_3^-}$, and (c) N^* in the density range of 26.5 to 27.5 kg m^{-3} at 40°S (blue) and 30°N (orange) in the Atlantic basin. In Figures 6a and 6b, the values from this study at 40°S are compared to data from 30°N [Knapp *et al.*, 2008]. In Figure 6c, N^* concentrations are calculated from GEOSECS data. (d) The concentration of remineralized NO_3^- added to the thermocline along isopycnals is calculated at 30°N. The blue circles indicate the calculation of remineralized NO_3^- concentration using apparent oxygen utilization assuming a nutrient remineralization stoichiometry of $-150:16:1$ ($\text{NO}_{3\text{remin}} = (1/150 \times \text{AOU}) \times 16$). Remineralized NO_3^- is also estimated by using the modification of $\delta^{18}\text{O}_{\text{NO}_3^-}$ from 40°S to 30°N. This is calculated by $\delta^{18}\text{O}_{\text{meas}} = \delta^{18}\text{O}_{\text{nit}} \times (X) + \delta^{18}\text{O}_{\text{imported}} \times (1 - X)$. The green, red, and orange crosses indicate the calculated values using $\delta^{18}\text{O}_{\text{nit}}$ values of 1.4‰, 1.6‰, and 1.8‰, respectively. (e) The proportion of NO_3^- which has undergone recycling between 40°S and 30°N is calculated by $\text{NO}_{3\text{remin}}/\text{NO}_{3\text{total}}$. (f) The nutrient stoichiometry of remineralized N:P is calculated by comparing remineralized NO_3^- estimates to remineralized PO_4^{3-} ($1/150 \times \text{AOU}$). The blue dashed line shows the 16:1 stoichiometry assumed from nutrient remineralization concomitant with O_2 consumption.

Modification of this signature during transit within the Atlantic can be tracked by comparing $\delta^{18}\text{O}_{\text{NO}_3^-}$ in water masses at 40°S with the same density at 30°N [Knapp *et al.*, 2008]. The North Atlantic subtropical water masses have a lower range of $\delta^{18}\text{O}_{\text{NO}_3^-}$ of 1.8 to 2.6‰ over the same density range (Figure 6). The $\delta^{18}\text{O}_{\text{NO}_3^-}$ changes implicate upward mixing and algal consumption converting preformed NO_3^- into regenerated NO_3^- during passage through the low-latitude Atlantic. These processes of supply, uptake by phytoplankton, and regeneration lead to the loss of isotopic enrichment evidenced at 40°S as the intermediate waters circulate in the Atlantic.

The supply of nutrients to the low-latitude thermocline has been investigated in previous work through the use of respiration stoichiometry [e.g., Kaehler *et al.*, 2010]. The consumption of O_2 in the process of respiration and nutrient production can indicate the extent of nutrient uptake and remineralization. This technique has limitations as the nutrient stoichiometry of $\text{O}_2:\text{NO}_3^-:\text{PO}_4^{3-}$ is only assumed. To assess the subtropical cycling of nutrients, an estimation of the change in the proportion of remineralized: total NO_3^- between 40°S and 30°N can be calculated by two separate approaches, using first stoichiometric and second isotopic estimates (Figure 6). For stoichiometric estimates, preformed and remineralized NO_3^- were calculated using AOU based on oxygen saturation [Garcia and Gordon, 1992] and a nutrient stoichiometry of $\text{O}_2:\text{NO}_3^-:\text{PO}_4^{3-} = -150:16:1$ [Anderson, 1995]. An average remineralized NO_3^- of 4.6 mmol m^{-3} was calculated using Geochemical Ocean Sections Study (GEOSECS) data from 40°S to 30°N between 26.4 and 27.1 kg m^{-3} .

The degree of recycling determined by $\delta^{18}\text{O}_{\text{NO}_3^-}$ is dependent on the $\delta^{18}\text{O}_{\text{NO}_3^-}$ of newly nitrified NO_3^- (denoted $\delta^{18}\text{O}_{\text{nit}}$) produced and is independent of assumed nutrient stoichiometry. As NO_3^- is consumed by phytoplankton, this process acts as an ultimate loss of the O from fixed N. During the process of nitrification, $\delta^{18}\text{O}$ “resets” to lower values of $\sim 1.1\text{‰}$ plus $\delta^{18}\text{O}_{\text{H}_2\text{O}}$ [Sigman *et al.*, 2009a]. In the subtropical Atlantic surface waters, the $\delta^{18}\text{O}$ of water ranges between 0.3 and 1.5‰ [Bigg and Rohling, 2000]. This would suggest that the newly nitrified NO_3^- produced within the subtropical Atlantic would obtain a $\delta^{18}\text{O}_{\text{nit}}$ of 1.4 to 2.6‰. To investigate nutrient supply and modification through the subtropics, three conservative estimates of $\delta^{18}\text{O}_{\text{nit}}$ have been used (1.4, 1.6, and 1.8‰, see Table 2). The recycling efficiency of NO_3^- was estimated by calculating the necessary amount of nitrification required to decrease $\delta^{18}\text{O}_{\text{NO}_3^-}$ to the measured signature at 30°N ($\delta^{18}\text{O}_{\text{meas}} = \delta^{18}\text{O}_{\text{nit}} \times (X) + \delta^{18}\text{O}_{\text{imported}} \times (1 - X)$).

Table 2. Estimations of Remineralized NO_3^- Using AOU and $\delta^{18}\text{O}_{\text{NO}_3}$ in the Water Density Range of 26.4 to 27.1 kg m^{-3} ^a

Method	$\delta^{18}\text{O}_{\text{nit}}$ (‰)	Remineralized NO_3^- (mmol m^{-3})	Excess N above Redfield (mmol m^{-3})	N:P	New N estimate Using $\delta^{18}\text{O}_{\text{NO}_3}$ (%)
AOU	n/a	4.6	n/a	16	n/a
$\delta^{18}\text{O}$	1.4	5.1	0.5	17.9	12
$\delta^{18}\text{O}$	1.6	5.5	0.9	19.2	20
$\delta^{18}\text{O}$	1.8	6.0	1.4	20.8	30

^aThe AOU value is compared to various $\delta^{18}\text{O}_{\text{nit}}$ estimates to calculate the N:P stoichiometry and new N estimates.

Although both approaches estimate remineralization, it is important to note that the absolute estimates of regenerated nitrate can be underestimated as the SAMW/AAIW undergo mixing from the South to the North Atlantic as can be identified with increases in temperature between these two regions (supporting information). This mixing with shallower waters decreases NO_3^- concentration and increases oxygen and could decouple the linear relationship between AOU and nitrate concentrations. In the supporting information, we show that the relationship between AOU and nitrate concentrations is linear at intermediate depths despite mixing. Therefore, this artifact should not affect the comparisons made below between the two approaches.

The estimations from the two methods show a large discrepancy in the proportion of remineralized NO_3^- at 30°N between a density range of 26.7 and 27.1 kg m^{-3} (Table 2 and Figure 5). Irrespective of $\delta^{18}\text{O}_{\text{nit}}$ used, the isotopic estimates suggest that a larger proportion of the NO_3^- pool is regenerated compared to the stoichiometric approach (Table 2). In Table 2, the estimates of excess N above the AOU estimates are calculated for each of the $\delta^{18}\text{O}_{\text{nit}}$ estimates. Here we estimate an increase in remineralized NO_3^- of between 0.5 and 1.4 mmol m^{-3} above the AOU estimate of 4.6 mmol m^{-3} . Apparent oxygen utilization assumes a ratio of 16:1 for N:P remineralization; however, $\delta^{18}\text{O}_{\text{NO}_3}$ -based estimates do not rely on assumed nutrient stoichiometry and calculate the amount of NO_3^- which has been nitrified from organic matter. The estimate from these approaches can be reconciled if N:P ratios of regeneration were higher (18–21:1). This reasoning provides a mechanism for investigating nutrient remineralization stoichiometry, as the decoupling suggests an underestimation of N:P using AOU methods. This suggests that the Atlantic organic matter N:P remineralization stoichiometry, integrated over 40°S–30°N, is higher than Redfield ratios. The excess N above Redfield which is added to the Atlantic thermocline is estimated between 12 and 30% of NO_3^- in this density range (Table 2).

The $\delta^{15}\text{N}_{\text{NO}_3}$ can be used to determine the underlying reasons for higher N:P stoichiometry. If no new N is added to the water masses in transit, then there should be no change in the $\delta^{15}\text{N}$ signatures (Figure 6). The lower $\delta^{15}\text{N}_{\text{NO}_3}$ at 30°N suggests an external source of isotopically light N being added to the water column. To calculate the required addition of new N to decrease $\delta^{15}\text{N}_{\text{NO}_3}$, we can calculate the proportion of newly fixed N required at each density ($\delta^{15}\text{N}_{\text{meas}} = \delta^{15}\text{N}_{\text{new}} \times (X) + \delta^{15}\text{N}_{\text{imported}} \times (1 - X)$). This approach is similar to previous methods of estimating new N addition to the Atlantic via isotope mass balance [Knapp *et al.*, 2008]. We calculate 12–17% of NO_3^- within this density range and added this to subtropical Atlantic from a source with isotopic composition of –1‰. This estimate of new N addition falls within our $\delta^{18}\text{O}_{\text{nit}}$ estimates and gives confidence to our assumptions of a considerable input of new N driving a change in the N:P stoichiometry (Table 2). Using both $\delta^{15}\text{N}$ and $\delta^{18}\text{O}$, we have demonstrated that an external source of isotopically light N is required to reconcile both the $\delta^{15}\text{N}$ and $\delta^{18}\text{O}$ budgets for the subtropical Atlantic.

A difference in N* of 3.3 μM has been calculated between the water masses entering and leaving the Atlantic basin, which would suggest an Atlantic N:P ratio of 19.3:1 [Moore *et al.*, 2009], and this high N:P stoichiometry is within our estimates of NO_3^- input to the thermocline. A study of NO_3^- isotope signatures in the North Atlantic similarly concluded inputs of new N to the Atlantic thermocline [Knapp *et al.*, 2008]. This study further concludes that the high N:P stoichiometry and low- $\delta^{15}\text{N}$ source are added to the thermocline through remineralization. Phytoplankton, other than diazotrophs, cannot produce isotopically light N in the tropics and subtropics where NO_3^- consumption is near complete in surface waters. Integrated over large temporal and spatial scales, their sinking remains are expected to conform to Redfield stoichiometry. Atmospheric deposition can be a source of isotopically light N to the surface waters, but it is unlikely to produce high N:P stoichiometry in sinking particles and during remineralization at depths. This is because N released from the solubilization of dust at the surface needs to be transported to depth through biological uptake,

sinking, and remineralization and hence is expected to follow Redfield Stoichiometry. Therefore, N_2 fixation is the only process which is likely to produce isotopically light N as well as high N:P ratios during regeneration of sinking detritus at intermediate depths.

In summary, we estimate using $\delta^{18}O$ higher concentrations of remineralized NO_3^- in the subtropics than calculate using AOU concentrations. The NO_3^- carried through intermediate waters undergoes substantial recycling in the Atlantic thermocline. In addition, the modification of $\delta^{15}N_{NO_3}$ and $\delta^{18}O_{NO_3}$ and the inferred high N:P ratios of regenerated nutrients suggest a significant addition of new N by diazotrophs. This modification of the subtropical intermediate waters strongly suggests that the high N:P of nutrients is caused by the remineralization of high N:P detritus and that a significant component of this is from new N input by diazotrophs.

4.3. Export of Low $\delta^{15}N$ and $\delta^{18}O$ Nitrate to the Global Ocean From the Atlantic Basin

The NADW is principally formed from the Southern Ocean water masses which are transported northward through the South Atlantic feeding NADW formation in the North Atlantic (~ 21.5 sverdrup (Sv)). The NADW nutrient properties should therefore reflect the integrated product of NO_3^- from the subtropical Atlantic thermocline and the deepwater sources which supply its formation. This can be investigated by comparing the NADW to the isotopic signatures of the AABW and intermediate waters. Here we use 16 Sv for the influx of intermediate waters, 5.5 Sv for the AABW, and 20 Sv for the export of NADW (as used by Moore *et al.* [2009] from 30°S in the South Atlantic). From these estimates, the AABW and AAIW comprise approximately 25% and 75% of the NADW volume, converting to 70% and 30% of the preformed NO_3^- component.

Using $\delta^{18}O_{NO_3}$ of these water masses at 40°S (intermediate waters = 2.9‰, AABW = 2.0‰), we can calculate the expected $\delta^{18}O_{NO_3}$ exported from the Atlantic NADW but ignoring the effects of nutrient recycling within the Atlantic. This would produce $\delta^{18}O_{NO_3}$ of newly formed NADW of ~ 2.3 ‰, which is higher than the average value of 2.0‰ measured at 40°S as it is exported to the Southern Ocean. The process of recycling NO_3^- through the low-latitude Atlantic therefore decreases deepwater $\delta^{18}O_{NO_3}$ in the NADW by ~ 0.3 ‰. It can be inferred that the addition of low $\delta^{15}N_{NO_3}$ to the low-latitude Atlantic also decreases NADW $\delta^{15}N_{NO_3}$. We estimate that the NADW $\delta^{15}N_{NO_3}$ would be 5.1‰ from the mixing of 40°S water mass sources (intermediate waters = 6.1‰, AABW = 4.8‰). Instead, the addition of new N in the low-latitude Atlantic lowers $\delta^{15}N_{NO_3}$ of the upper MOC, thereby decreasing NADW $\delta^{15}N_{NO_3}$ to 4.8‰. We therefore can identify the importance of recycling processes and diazotrophy within the subtropical Atlantic in determining the NO_3^- isotopic signatures in the NADW.

Figure 7 provides a global perspective of deepwater mass pathways and the communication between N_2 fixation and water column denitrification in the global ocean. Each of the three ocean basins is fed with NO_3^- of relatively high $\delta^{15}N_{NO_3}$ and $\delta^{18}O_{NO_3}$ through intermediate and mode waters that are ventilated in the Southern Ocean and have experienced partial biological utilization. These isotopic signatures are modified by nutrient cycling processes within each of the ocean basins, and the outflowing deep waters reflect these processes. In this study, we observe modifications in NO_3^- isotope signatures within Southern Ocean intermediate water masses as they move through the low-latitude Atlantic Ocean. The lowering of $\delta^{18}O_{NO_3}$ between 40°S and 30°N indicates an increase in the proportion of remineralized NO_3^- in intermediate waters as they transit the low-latitude Atlantic. As NO_3^- is mixed to the surface layer, taken up by phytoplankton, and remineralized, there is a fortification of N (relative to P and oxygen consumption and an increase in N^*) in remineralized nutrients added to the water column. Simultaneously, there is a lowering of $\delta^{15}N_{NO_3}$, indicating the addition of new N with lower $\delta^{15}N_{NO_3}$. This suggests that organic matter remineralized in the low-latitude Atlantic has a N:P ratio higher than classical Redfield N:P stoichiometry [Redfield, 1958] and lower in $\delta^{15}N_{NO_3}$. This we attribute to N_2 fixation in the low latitude Atlantic, providing a source of low $\delta^{15}N_{NO_3}$ and excess N which is exported by NADW to the Southern Ocean feeding the global ocean. Our observations are consistent with recent suggestions that large-scale transport of excess P drives Atlantic N_2 fixation [Straub *et al.*, 2013]. We estimate that this process accounts for 12–30% of NO_3^- (section 4.2) that is added to the subtropical Atlantic above 27.1 kg m^{-3} . N_2 fixation in the Atlantic is estimated to only account for $\sim 15\%$ of global N_2 fixation [Deutsch *et al.*, 2007; Moore *et al.*, 2009]. Although the majority of N_2 fixation is likely to occur in the Pacific and Indian Oceans, the Atlantic is unique as a source of excess N to the global ocean exported through the NADW.

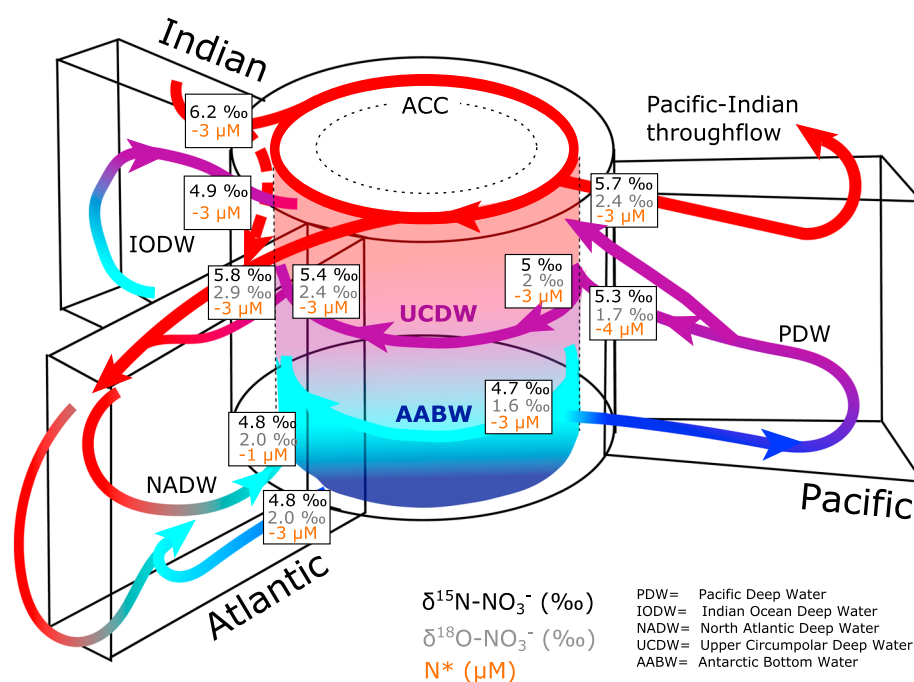


Figure 7. A generalized schematic of water mass pathways and communication between regions of denitrification and N_2 fixation in the global ocean. The $\delta^{15}\text{N}_{\text{NO}_3}$ in deepwater masses exported out of the ocean basins may reflect the balance between N_2 fixation and water column denitrification (2500 m at 40°S ; Atlantic = 4.8‰ , Indian = 4.9‰ , and Pacific = 5.3‰). In contrast, similar $\delta^{18}\text{O}_{\text{NO}_3}$ in deepwater masses reflect nitrification which resets $\delta^{18}\text{O}_{\text{NO}_3}$ closer to $\delta^{18}\text{O}_{\text{H}_2\text{O}} + 1.1\text{‰}$. The Southern Ocean acts as a mixer for these signatures with mean isotopic signatures of $\delta^{15}\text{N}_{\text{NO}_3} = 4.7\text{--}5.4\text{‰}$ and $\delta^{18}\text{O}_{\text{NO}_3} = 1.6\text{--}2.1\text{‰}$ [Difiore et al., 2006; Sigman et al., 2009a; Rafter et al., 2013, this study], and the UCDW shows variability in $\delta^{15}\text{N}_{\text{NO}_3}$ reflecting this mixing process.

In contrast to the Atlantic waters examined in this study, the Pacific Deep Water (PDW) has higher $\delta^{15}\text{N}_{\text{NO}_3}$ signatures. This reflects the importance of water column denitrification which is prevalent in the large ODZs of the eastern Pacific. As a consequence, the PDW supplies the Southern Ocean with NO_3^- that is $\sim 0.5\text{‰}$ heavier in $\delta^{15}\text{N}_{\text{NO}_3}$ relative to the NADW, with low N^* values indicating an N deficit from denitrification [Rafter et al., 2013]. Although isotopic studies of the Indian Ocean Deep Water are currently sparse, available data indicate that $\delta^{15}\text{N}_{\text{NO}_3}$ values of this water mass fall between those of the Pacific and Atlantic (Figure 7). Thus, the distinct $\delta^{15}\text{N}_{\text{NO}_3}$ properties and nutrient stoichiometry for deepwater export from the three basins at 40°S reflect the relative degree of imbalance in N_2 fixation and denitrification within these basins.

The Southern Ocean acts as a mixer of deep waters with distinct isotopic signatures and nutrient stoichiometry (Figure 7). Of particular importance is the UCDW which receives deep waters from all three ocean basins and as a result exhibits high nutrient concentrations and old ^{14}C ages [England, 1995]. The Atlantic UCDW retains a signature of denitrification, with high $\delta^{15}\text{N}_{\text{NO}_3}$ and low N^* , which is also evident in the SE Pacific sector of the Southern Ocean (Figure 7) [Sigman et al., 2000]. At 40°S , the UCDW has an initial N^* concentration of $-3.6\text{ }\mu\text{M}$ at 1500 m, suggesting an $\sim 3.6\text{ }\mu\text{mol L}^{-1}$ deficiency in N relative to P. This indicates that neither an isotopic nor stoichiometric balance is achieved during Southern Ocean mixing processes, but this balance remains in favor of high $\delta^{15}\text{N}_{\text{NO}_3}$ and excess P. Importantly, this suggests that the export of excess N from the Atlantic fails to fully compensate for the N deficit in Indo-Pacific deep waters which generate excess P after mixing in the Southern Ocean. This has important implications for water mass pathways through which denitrification and N_2 fixation are coupled in the ocean and the balancing of marine fixed N inventory.

The UCDW upwells at the Polar Front forming the upper ACC and subsequently feeds intermediate and mode waters (Figure 7). Mode and intermediate waters sourced from the UCDW are the primary suppliers of nutrients to the subtropics accounting for $\sim 75\%$ of nutrients to subtropical export production [Palter et al., 2010]. Although isotopic signatures of intermediate and mode waters are modified after upwelling through partial NO_3^- utilization and mixing processes in the Southern Ocean (as discussed in section 4.1), they retain the N

deficit inherited from the UCDW. These Southern Ocean intermediate water masses are globally significant in supplying excess P to the subtropical thermocline. This preconditions the world's subtropical surface ocean to be N limited favoring N_2 fixation. This explains why N_2 fixation can be supported in all three major ocean basins and even in the Atlantic, where minimal N loss is occurring locally.

This water mass pathway linking deep waters of the ocean with thermocline waters through the Southern Ocean suggests that the mass balance in the global N cycle and the near conformity to Redfield ratio can be only achieved on time scales of ocean circulation (~900 years) [Matsumoto, 2007]. Global atmospheric N input to the ocean from anthropogenic sources may account for ~1/3 of external fixed N supply, highlighting the significant increases in N supply to the global ocean [Duce *et al.*, 2008]. In addition, expansion of ODZs due to climate warming is expected to increase ocean denitrification [Bopp *et al.*, 2002; Kalvelage *et al.*, 2013]. Our study suggests that the consequences of such large-scale perturbations to N inputs and outputs will persist on longer time scales of ocean circulation before the N cycle is balanced, having a global impact on oceanic N:P stoichiometry.

5. Conclusions

This study presents a comprehensive set of NO_3^- isotope data from the South Atlantic, allowing the communication of N cycling processes between the Atlantic basin and the global ocean to be investigated. The intermediate waters which enter the Atlantic are formed from the UCDW, which carries slightly enriched signatures from denitrification regions in the Pacific. The AAIW NO_3^- isotope properties can be simply explained by nutrient utilization in surface waters at the Polar Front, and the SAMW is further influenced by mixing with subtropical waters farther to the north. These water masses transport enriched $\delta^{15}N_{NO_3}$ and $\delta^{18}O_{NO_3}$ and low-N* waters into the low-latitude Atlantic.

The modification of intermediate waters can be identified by decreases in $\delta^{15}N_{NO_3}$ and $\delta^{18}O_{NO_3}$ from 40°S to 30°N. Using $\delta^{18}O_{NO_3}$ and nutrient stoichiometry, we can identify a fortification in N over P in the intermediate waters of the subtropical Atlantic. The modification of $\delta^{15}N_{NO_3}$ and $\delta^{18}O_{NO_3}$ and the inferred high N:P ratios of regenerated nutrients suggest significant addition of new N by diazotrophs. These modified intermediate waters supply NADW formation and have low $\delta^{15}N_{NO_3}$ and high N:P ratios in comparison to the PDW.

Globally, the export of excess N through NADW fails to fully compensate for the N deficit in the Indo-Pacific deep waters resulting in the generation excess P after mixing and upwelling in the Southern Ocean. We speculate that this may drive the observed widespread N limitation and N_2 fixation in the world's ocean as Southern Ocean-sourced intermediate waters ventilate the thermoclines of the three ocean basins. The water mass pathway identified here linking areas of N loss to the subtropical thermocline waters routed through the Southern Ocean suggests that balancing the oceanic N cycle after any large-scale perturbation in sources and sinks can only be achieved on time scales of ocean circulation.

Acknowledgments

We thank the crew and scientists of the RRS *Discovery* (D357) and RRS *James Cook* (JC068), Gideon Henderson for coordination of UK GEOTRACES 40°S transect, Sue Reynolds and Amandine Sabadel for nutrient analyses, and Colin Chilcott for assistance with isotope analyses at the University of Edinburgh. We further acknowledge Karen Casciotti and Jan Kaiser for generously sharing their expertise on the denitrifier method. This work was funded by the UK GEOTRACES National Environment Research Council (NERC) consortium grant (NE/H008497/1/NERC) which included a studentship for R. E. Tuerena. All data used are freely available on request from R.E.T. (Robyn.Tuerena@liverpool.ac.uk). Nitrate isotope data have further been submitted to British Oceanographic Data Centre as part of the UK GEOTRACES data set.

References

- Altabet, M. A., and R. Francois (2001), Nitrogen isotope biogeochemistry of the antarctic polar frontal zone at 170°W, *Deep Sea Res., Part II*, 48(19–20), 4247–4273.
- Altabet, M. A., C. Pilskaln, R. Thunell, C. Pride, D. Sigman, F. Chavez, and R. Francois (1999), The nitrogen isotope biogeochemistry of sinking particles from the margin of the eastern North Pacific, *Deep Sea Res., Part I*, 46(4), 655–679.
- Anderson, L. A. (1995), On the hydrogen and oxygen content of marine phytoplankton, *Deep Sea Res., Part I*, 42(9), 1675–1680.
- Bigg, G. R., and E. J. Rohling (2000), An oxygen isotope data set for marine waters, *J. Geophys. Res.*, 105(C4), 8527–8535, doi:10.1029/2000JC900005.
- Böhlke, J. K., S. J. Mroczkowski, and T. B. Coplen (2003), Oxygen isotopes in nitrate: New reference materials for 18O: 17O: 16O measurements and observations on nitrate-water equilibration, *Rapid Commun. Mass Spectrom.*, 17(16), 1835–1846.
- Bopp, L., C. Le Quere, M. Heimann, A. C. Manning, and P. Monfray (2002), Climate-induced oceanic oxygen fluxes: Implications for the contemporary carbon budget, *Global Biogeochem. Cycles*, 16(2), 1022, doi:10.1029/2001GB001445.
- Boyd, P. W., et al. (2007), Mesoscale iron enrichment experiments 1993–2005: Synthesis and future directions, *Science*, 315(5812), 612–617.
- Brandes, J. A., and A. H. Devol (2002), A global marine fixed-nitrogen isotopic budget: Implications for Holocene nitrogen cycling, *Global Biogeochem. Cycles*, 16(4), 1120, doi:10.1029/2001GB001856.
- Brandes, J. A., A. H. Devol, T. Yoshinari, D. A. Jayakumar, and S. W. A. Naqvi (1998), Isotopic composition of nitrate in the central Arabian Sea and eastern tropical North Pacific: A tracer for mixing and nitrogen cycles, *Limnol. Oceanogr.*, 43(7), 1680–1689.
- Buchwald, C., A. E. Santoro, M. R. McIlvin, and K. L. Casciotti (2012), Oxygen isotopic composition of nitrate and nitrite produced by nitrifying cocultures and natural marine assemblages, *Limnol. Oceanogr.*, 57(5), 1361–1375.
- Carpenter, E. J., H. R. Harvey, B. Fry, and D. G. Capone (1997), Biogeochemical tracers of the marine cyanobacterium *Trichodesmium*, *Deep Sea Res., Part I*, 44(1), 27–38.
- Carritt, D. E., and J. H. Carpenter (1966), Comparison and evaluation of currently employed modifications of the Winkler method for determining dissolved oxygen in seawater; a NASCO report, *J. Mar. Res.*, 24, 286–318.

- Casciotti, K. L., D. M. Sigman, M. G. Hastings, J. K. Bohlke, and A. Hilkert (2002), Measurement of the oxygen isotopic composition of nitrate in seawater and freshwater using the denitrifier method, *Anal. Chem.*, **74**(19), 4905–4912.
- Dehaers, F., F. Fripiat, A. Cavagna, T. Trull, C. Fernandez, D. Davies, A. Roukaerts, D. Fonseca Batista, F. Planchon, and M. Elskens (2015), Nitrogen cycling in the Southern Ocean Kerguelen Plateau area: Evidence for significant surface nitrification from nitrate isotopic compositions, *Biogeosciences*, **12**(5), 1459–1482.
- Deutsch, C., J. L. Sarmiento, D. M. Sigman, N. Gruber, and J. P. Dunne (2007), Spatial coupling of nitrogen inputs and losses in the ocean, *Nature*, **445**(7124), 163–167.
- DiFiore, P. J., D. M. Sigman, T. W. Trull, M. J. Lourey, K. Karsh, G. Cane, and R. Ho (2006), Nitrogen isotope constraints on subantarctic biogeochemistry, *J. Geophys. Res.*, **111**, C08016, doi:10.1029/2005JC003216.
- DiFiore, P. J., D. M. Sigman, and R. B. Dunbar (2009), Upper ocean nitrogen fluxes in the Polar Antarctic Zone: Constraints from the nitrogen and oxygen isotopes of nitrate, *Geochem. Geophys. Geosyst.*, **10**, Q11016, doi:10.1029/2009GC002468.
- Duce, R. A., et al. (2008), Impacts of atmospheric anthropogenic nitrogen on the open ocean, *Science*, **320**(5878), 893–897.
- England, M. H. (1995), The age of water and ventilation time scales in a global ocean model, *J. Phys. Oceanogr.*, **25**(11), 2756–2777.
- Garcia, H. E., and L. I. Gordon (1992), Oxygen solubility in seawater: Better fitting equations, *Limnol. Oceanogr.*, **37**, 1307–1312.
- Granger, J., D. M. Sigman, J. A. Needoba, and P. J. Harrison (2004), Coupled nitrogen and oxygen isotope fractionation of nitrate during assimilation by cultures of marine phytoplankton, *Limnol. Oceanogr.*, **49**(5), 1763–1773.
- Gruber, N. (2004), The dynamics of the marine nitrogen cycle and atmospheric CO₂, in *Carbon Climate Interactions*, edited by T. Ogunz and M. Follows, pp. 97–148, Kluwer, Dordrecht.
- Gruber, N., and J. L. Sarmiento (1997), Global patterns of marine nitrogen fixation and denitrification, *Global Biogeochem. Cycles*, **11**, 235–266, doi:10.1029/97GB00077.
- Hydes, D. J., et al. (2010), Determination of dissolved nutrients (N, P, Si) in seawater with high precision and inter-comparability using gas-segmented continuous flow analysers, *The Go-ship Repeat Hydrography Manual: A Collection of Expert Reports and Guidelines*, UNESCO-IOC, IOCCP Rep., **14**(134).
- Jenkins, W. J., and S. C. Doney (2003), The subtropical nutrient spiral, *Global Biogeochem. Cycles*, **17**(4), 1110, doi:10.1029/2003GB002085.
- Kaehler, P., A. Oschlies, H. Dietze, and W. Koeve (2010), Oxygen, carbon, and nutrients in the oligotrophic eastern subtropical North Atlantic, *Biogeosciences*, **7**(3), 1143–1156.
- Kalvelage, T., G. Lavik, P. Lam, S. Contreras, L. Arteaga, C. R. Loscher, A. Oschlies, A. Pailmier, L. Stramma, and M. M. M. Kuypers (2013), Nitrogen cycling driven by organic matter export in the South Pacific oxygen minimum zone, *Nat. Geosci.*, **6**, 228–234, doi:10.1038/ngeo1739.
- Karsh, K. L., J. Granger, K. Kritee, and D. M. Sigman (2012), Eukaryotic assimilatory nitrate reductase fractionates N and O isotopes with a ratio near unity, *Environ. Sci. Technol.*, **46**(11), 5727–5735.
- Knapp, A. N., P. J. DiFiore, C. Deutsch, D. M. Sigman, and F. Lipschultz (2008), Nitrate isotopic composition between Bermuda and Puerto Rico: Implications for N₂ fixation in the Atlantic Ocean, *Global Biogeochem. Cycles*, **22**, GB3014, doi:10.1029/2007GB003107.
- Matsumoto, K. (2007), Radiocarbon-based circulation age of the world oceans, *J. Geophys. Res.*, **112**, C09004, doi:10.1029/2007JC004095.
- McIlvin, M. R., and K. L. Casciotti (2011), Technical updates to the bacterial method for nitrate isotopic analyses, *Anal. Chem.*, **83**(5), 1850–1856.
- Moore, C. M., et al. (2009), Large-scale distribution of Atlantic nitrogen fixation controlled by iron availability, *Nat. Geosci.*, **2**(12), 867–871.
- Naveira Garabato, A. C., E. L. McDonagh, D. P. Stevens, K. J. Heywood, and R. J. Sanders (2002), On the export of Antarctic Bottom Water from the Weddell Sea, *Deep Sea Res., Part II*, **49**(21), 4715–4742.
- Orsi, A. H., G. C. Johnson, and J. L. Bullister (1999), Circulation, mixing, and production of Antarctic Bottom Water, *Prog. Oceanogr.*, **43**(1), 55–109.
- Oudot, C., J. F. Terner, C. Andrieu, E. S. Braga, and P. Morin (1999), On the crossing of the equator by intermediate water masses in the western Atlantic Ocean: Identification and pathways of Antarctic Intermediate Water and Upper Circumpolar Water, *J. Geophys. Res.*, **104**(C9), 20,911–20,926, doi:10.1029/1999JC900123.
- Palter, J. B., J. L. Sarmiento, A. Gnanadesikan, J. Simeon, and R. D. Slater (2010), Fueling export production: Nutrient return pathways from the deep ocean and their dependence on the Meridional Overturning Circulation, *Biogeosciences*, **7**(11), 3549–3568.
- Piola, A. R., and D. T. Georgi (1982), Circumpolar properties of Antarctic Intermediate Water and Subantarctic Mode Water, *Deep Sea Res., Part A*, **29**(6), 687–711.
- Rafter, P. A., P. J. DiFiore, and D. M. Sigman (2013), Coupled nitrate nitrogen and oxygen isotopes and organic matter remineralization in the Southern and Pacific Oceans, *J. Geophys. Res. Oceans*, **118**, 4781–4794, doi:10.1002/jgrc.20316.
- Redfield, A. C. (1958), The biological control of chemical factors in the environment, *Am. Sci.*, **46**, 205–221.
- Sarmiento, J. L., N. Gruber, M. A. Brzezinski, and J. P. Dunne (2004), High-latitude controls of thermocline nutrients and low latitude biological productivity, *Nature*, **427**(6969), 56–60.
- Sigman, D. M., M. A. Altabet, D. C. McCorkle, R. Francois, and G. Fischer (2000), The delta N-15 of nitrate in the Southern Ocean: Nitrogen cycling and circulation in the ocean interior, *J. Geophys. Res.*, **105**(C8), 19,599–19,614, doi:10.1029/2000JC000265.
- Sigman, D. M., K. L. Casciotti, M. Andreani, C. Barford, M. Galanter, and J. K. Bohlke (2001), A bacterial method for the nitrogen isotopic analysis of nitrate in seawater and freshwater, *Anal. Chem.*, **73**(17), 4145–4153.
- Sigman, D. M., J. Granger, P. J. DiFiore, M. M. Lehmann, R. Ho, G. Cane, and A. van Geen (2005), Coupled nitrogen and oxygen isotope measurements of nitrate along the eastern North Pacific margin, *Global Biogeochem. Cycles*, **19**, GB4022, doi:10.1029/2005GB002458.
- Sigman, D. M., P. J. DiFiore, M. P. Hain, C. Deutsch, Y. Wang, D. M. Karl, A. N. Knapp, M. F. Lehmann, and S. Pantoja (2009a), The dual isotopes of deep nitrate as a constraint on the cycle and budget of oceanic fixed nitrogen, *Deep Sea Res., Part I*, **56**(9), 1419–1439.
- Sigman, D. M., P. J. DiFiore, M. P. Hain, C. Deutsch, and D. M. Karl (2009b), Sinking organic matter spreads the nitrogen isotope signal of pelagic denitrification in the North Pacific, *Geophys. Res. Lett.*, **36**, L08605, doi:10.1029/2008GL035784.
- Sloyan, B. M., and S. R. Rintoul (2001), Circulation, renewal, and modification of Antarctic mode and intermediate water, *J. Phys. Oceanogr.*, **31**(4), 1005–1030.
- Smart, S. M., S. E. Fawcett, S. J. Thomalla, M. A. Weigand, C. J. C. Reason, and D. M. Sigman (2015), Isotopic evidence for nitrification in the Antarctic winter mixed layer, *Global Biogeochem. Cycles*, **29**, 427–445, doi:10.1002/2014GB005013.
- Stramma, L., and M. H. England (1999), On the water masses and mean circulation of the South Atlantic Ocean, *J. Geophys. Res.*, **104**(C9), 20,863–20,883, doi:10.1029/1999JC900139.
- Straub, M., D. M. Sigman, H. Ren, A. Martinez-Garcia, A. N. Meckler, M. P. Hain, and G. H. Haug (2013), Changes in North Atlantic nitrogen fixation controlled by ocean circulation, *Nature*, **501**, 200–203.
- Talley, L. D. (1996), Antarctic Intermediate Water in the South Atlantic, in *South Atlantic: Present and Past Circulation*, pp. 219–238, Springer, Berlin.

- Toggweiler, J. R., K. Dixon, and W. S. Broecker (1991), The Peru upwelling and the ventilation of the South Pacific thermocline, *J. Geophys. Res.*, **96**(C11), 20,467–20,497, doi:10.1029/91JC02063.
- Weber, T., and C. Deutsch (2014), Local versus basin-scale limitation of marine nitrogen fixation, *Proc. Natl. Acad. Sci. U.S.A.*, **111**, 8741–8746.
- Woodward, E. M. S., and A. P. Rees (2001), Nutrient distributions in an anticyclonic eddy in the northeast Atlantic Ocean, with reference to nanomolar ammonium concentrations, *Deep Sea Res., Part II*, **48**, 775–793.